December 1985

LRP 281/85

ON THE DESIGN OF OPEN RESONATORS FOR QUASI-OPTICAL GYROTRONS

A. Perrenoud, M.Q. Tran and B. Isaak

ON THE DESIGN OF OPEN RESONATORS FOR QUASI-OPTICAL GYROTRONS

A. Perrenoud, M.Q. Tran and B. Isaak

Centre de Recherches en Physique des Plasmas

Association Euratom - Confédération Suisse

Ecole Polytechnique Fédérale de Lausanne

21, Av. des Bains, CH-1007 Lausanne / Switzerland

ABSTRACT

In the design of a 120 GHz 200 kW quasi-optical gyrotron, we have analyzed the influence of the open resonator geometry (two circular mirrors facing one another) on the electronic efficiency, the ohmic losses, the output coupling and the multimode behavior. The method used to optimize the resonator design will be presented. Mode selectivity is improved by using a resonator formed by two mirrors each of which has a central step. Numerical simulations show that single mode operation can also be attained in the more favorable situation of a magnetic field having a positive taper over the interaction region.

1. INTRODUCTION

The essential difference between conventional and quasi-optical gyrotrons resides in the resonator geometry. In a conventional gyrotron the electron beam is coaxial with a cylindrical cavity (which can be made of many tapered sections) whereas in the quasi-optical gyrotron the electron beam and the axis of a resonator formed by two spherical mirrors facing one another are perpendicular. In both concepts much effort is devoted to the calculation of the electromagnetic field modes inside the resonant structure and to the optimization of the electronic efficiency, while minimizing undesirable effects like mode mixing or ohmic losses. Because of its larger resonator, one advantage of the quasi-optical gyrotron [1] is the possibility of extrapolation towards the realization of the large units (150 GHz 1 MW) required for heating of nuclear fusion reactors.

Unfortunately the larger the resonator the more severe the problem of mode purity and mode competition becomes. Even if transverse TEM modes are suppressed because of their high diffraction losses, the number of longitudinal TEM_{00q} modes, which fall in the gyrotron instability bandwidth, is relatively large: more than ten for a 50 cm resonator at 120 GHz. The multimode behavior of quasi-optical gyrotrons has been studied [2] by performing self-consistent, time-dependent numerical simulations. Single mode operation can be attained in some cases, and depends strongly on the magnetic field (B) shaping. If B decreases over the interaction region, the more unstable modes grow first, destabilize higher frequency modes, and ultimately single mode operation is achieved. This is not the case for constant or increasing magnetic fields, which have higher electronic efficiencies. In the same article [2] it is also shown that a prebunching resonator increases both the mode selectivity and the efficiency of the device. This is the gyro-klystron concept.

It is the aim of this paper to report an alternative solution, the use of mirrors with a central step to increase the mode selectivity of single cavity gyrotrons. This study forms part of the design calculations for a 120 GHz, 200 kW quasi-optical gyrotron presently under construction at the CRPP.

2. QUASI-OPTICAL RESONATOR GEOMETRY

We consider here three symmetrical resonators: the first one (Fig. 1a) has conventional spherical mirrors while the other two possess a central step as depicted in Fig. 1b. The resonant structure of the latter two can thus be viewed as comprising two coaxial Fabry-Pérot resonators of different lengths.

The output coupling is achieved via annular slots. This solution is similar to the one adopted in the NRL quasi-optical gyrotron experiment [3], but in our case the power is equally coupled out from both sides of the resonator. This will alleviate the problems associated with the ceramic windows. The design parameters are summarized in Table 1 and discussed in the next section.

Parameter	Symbol	Resonator configuration (a) Without step	(b) 4λ step	(c) 5λ step
Resonator length	d	36	36	36
Mirror radius	a_m	6.5	7.0	7.0
Resonant wavelength	λ	0.2503	0.2503	0.2503
Transmission for mode q=287	T	0.04	0.04	0.04
Output coupling	ε	90.5	83.5	84.0
Diffraction quality factor	Q_{dif}	43800	44600	43600
Overall quality factor *	Q	41500	42300	41300
Spot size at electron beam #	w_o	0.99	1.02	1.02
Spot size at the mirror #	w_m	2.01	1.83	1.84

Table 1

Resonator Parameters for the $TEM_{0\ 0\ 287}$ mode

Lengths are in cm.

* Assuming gold-plated mirrors (conductivity $\sigma = 4.2 \cdot 10^7\ \Omega^{-1}m^{-1}$)

\# At the spot circumference the amplitude is 1/e of its value at the centre.

3. PHYSICAL CHARACTERISTICS OF THE RESONATOR

The calculation of the resonator properties for a given mode TEM_{00q} is based on Kirchhoff's formulation of the Huygens-Fresnel Principle. We have written a computer code [4] to compute the electric field profile on the mirror surfaces and along the electron beam path by adding the waves coming from both mirrors. Two important physical quantities can also be estimated:

T : the resonator's transmission

ε : the output coupling efficiency, defined as the ratio of the power diffracted through the slots divided by the total diffracted power.

The design parameters of both resonators have been determined by analyzing their influence on the gyrotron characteristics while keeping in mind the constraints of our experimental setup. The remainder of this section examines the significance of the parameters listed in Table 1, and discusses the choice of their values.

a) **Resonator length (d)**

A large resonator is preferable in order to decrease the ohmic heating per unit area of the mirror surface. However, the resonator and its coupling structure has to fit inside our vacuum vessel [5]. As a compromise we have set d = 36 cm.

b) **Longitudinal mode number (q)**

It is determined by the working frequency f = 120 GHz and the formulae

$$f = \frac{c}{2d}\left(q + \frac{1}{\pi}\,\mathrm{Arccos}(g)\right) \tag{1}$$

$$g = 1 - \frac{d}{R} \quad . \tag{2}$$

The resonant frequency depends only slightly on the curvature. For a confocal resonator (d = R), the nearest integer value deduced from Eq. (1) is q = 287. The electron beam is centered on a node of the electric field and its radius r_b has been chosen so as to maximize the annular beam efficiency in the linear regime. In the next sections (c-e), we will consider only the mode $TEM_{0\ 0\ 287}$.

c) **Spot size (w_o)**

To a close approximation, the spot size of the TEM_{00} mode depends on the mirror curvature according to

$$w_o = r_o \sqrt[4]{(1+g)/(1-g)} \tag{3}$$

where $r_o = \sqrt{d\lambda/2\pi}$. (4)

The spot size w_o is chosen so as to maximize the gyrotron electronic efficiency. For a 60 kV beam, the ratio w_o/λ should be close to 4.8 [2]. Using the electron beam parameters of Table 2, we note in Fig. 2 that η is not very strongly dependent on w_o as long as $3.8 < w_o/\lambda < 5.5$. Nevertheless, this restricts the range of g to $-0.45 < g < 0.30$.

Voltage		70 kV
$P_\perp/P_\parallel$		1.5
Mean radius (r_b)		2.0 mm
Maximum current		10 A
Pulse length	min.	50 μs
	max.	100 ms

Table 2:

Electron beam parameters of the CRPP gyrotron

d) **Output coupling efficiency (ε)**

To find an optimum ε is not easy because it is a function of four parameters: a_m, a_o, a_1, $|g|$. Figure 3 illustrates the variation of ε with $|g|$ when a_m and a_o are fixed and a_1 adjusted so that the resonator transmission has a given value (2 or 4%).

There is a noticeable variation of ε as a function of $|g|$. As pointed out in a previous paper [4], we see that confocal resonators have poor ε. We infer that $|g|$ should thus be chosen in the range $0.15 \leqslant |g| \leqslant 0.4$.

e) **Resonator transmission (T)**

The transmission influences two crucial gyrotron characteristics: the heat flux on the mirror and the operating point.

In steady state, the power transferred from the electron beam to the resonator field exactly compensates for the diffraction and ohmic losses. This means

$$\eta IV = P + L = 2\pi f \frac{W}{Q} \tag{5}$$

$$\frac{1}{Q} = \frac{1}{Q_{dif}} + \frac{1}{Q_{ohm}} \tag{6}$$

$$Q_{dif} = \frac{4\pi d f}{Tc} \tag{7}$$

$$Q_{ohm} = \frac{d}{2} \sqrt{\pi \mu_o f \sigma} \tag{8}$$

where
- P = diffracted power
- L = ohmic loss (heat flux)
- W = energy stored inside the resonator
- Q = Quality factor
- Q_{dif} = diffraction Q
- Q_{ohm} = ohmic Q ($\mu_o = 4\pi \cdot 10^{-7}$)
- σ = mirror conductivity at frequency f.

The ratio of the ohmic loss to the diffracted power is inversely proportional to T. From (7) and (8) we have:

$$\frac{L}{P} = \frac{Q_{dif}}{Q_{ohm}} = \frac{8}{Tc} \sqrt{\frac{\pi f}{\mu_o \sigma}} \tag{9}$$

If we take gold-plated mirrors, the low frequency conductivity $\sigma = 4.2 \cdot 10^7\ \Omega^{-1}m^{-1}$. For a T = 2% resonator and f = 120 GHz, L/P = 11.3%. For P = 200 kW, about 11 kW will be dissipated in each mirror. To enhance the global efficiency of the device and to simplify the technological problems associated with the removal of large heat flux, it is very important to maximize the transmission, while achieving an efficient operating point. Moreover, it is important to allow for a somewhat degraded Q_{ohm} due to surface imperfections [6].At 120 GHz it would be more realistic to consider a conductivity about 40% smaller than the low frequency value, leading to a heat flux approximately 20% higher.

The gyrotron operating point is characterised by E_C, the value of the RF electric field at the electron beam. For a given beam intensity and constant magnetic field, this point is found as the intersection of two curves (Fig. 4):

- $\eta(E_C)$ the electronic efficiency, calculated by integrating the electron trajectories in the interaction region using the actual electron beam parameters (Table 2).

- $(2\pi f/QIV)W(E_C)$ which is the power lost by the resonator divided by the beam power IV (Eq. 5). The resonator stored energy $W(E_C)$ is quadratic in E_C.

Let us study in more detail the case of a T = 0.02 resonator with g = -0.2. In order to find the overall maximum in efficiency we must also vary the static magnetic field profile. In Figures 5(a) to 5(f), we have plotted contours of $\eta(E_C, \Delta\omega/\omega)$ where the frequency mismatch is related to B by Eq. 10:

$$\frac{\Delta\omega}{\omega} = 1 - \frac{\Omega}{\gamma\omega} = 1 - \frac{eB}{2\pi m f \gamma} . \tag{10}$$

γ is the relativistic factor and is equal to 1.137 for V = 70 kV. B is the magnetic field at the centre of the resonator.

Also shown in Figs. 5(a) to 5(f) are the loci of the gyrotron operating points for various beam intensities. The overall maximum in efficiency tends to increase with the field taper. However, due to experimental constraints this taper in our gyrotron will be limited to 0.1 over 7.2 cm. We see from Fig. 5(e) that an efficiency of 30% can be achieved with a 5A-beam. From Eqs. (5) to (8), it can be seen that for our maximum beam current I = 10A the same operating point can be reached with T = 0.04. Therefore, we select T = 0.04.

From Fig. 3(b) we see that g = -0.3 maximizes the output coupling ε. Figure 6 shows the gyrotron operation point for the design parameters listed in Table 1.

f) **Mirror with a central step**

The optimization procedures of sections d) and e) have been repeated for the resonators with a central step. In addition, by varying the height and radius of the central step, we have tried to increase the diffraction losses of the $TEM_{00q\pm n}$ modes (q = 287) while keeping those of the TEM_{00q} around 4%. No systematic optimization of the design has yet been performed. The best set of parameters achieved so far is listed in Table 1. The radius of the central step (a_e) is such that about half of the e.m. field power is incident on it. The height (h) is approximately 4λ for resonator b and 5λ for resonator c. Table 3 lists the transmissions T of TEM_{00q} modes for q = 278 to 290. For the stepped resonators, it is seen that T increases rapidly with n as one moves away from the selected mode. This has a dramatic effect on the starting currents: the lower frequency modes (q = 279 to 282) can no longer be excited by a 10A beam.

Longitudinal mode q	Resonators (a) Without step T [%]	I [A]	η [%]	(b) With 4λ step T [%]	I [A]	(c) With 5λ step T [%]	I [A]
278	4.43	<0.	0.	50.0	<0.	62.0	<0.
279	4.38	10.	1.	44.1	100.	55.7	130.
280	4.33	4.9	4.	37.9	43.	48.9	55.0
281	4.28	1.8	10.	31.6	13.3	41.6	17.5
282	4.23	2.5	10.	25.4	15.0	33.9	20.0
283	4.18	1.5	17.5	19.4	7.0	26.1	9.4
284	4.13	2.6	15.5	13.8	8.7	18.6	11.7
285	4.09	2.0	30.	8.75	4.3	11.7	5.7
286	4.04	5.3	18.	5.40	7.1	6.43	8.5
→ 287	4.00	6.3	30.5	3.93	6.2	4.02	6.3
288	3.96	26.5	0.	5.50	37.	6.37	43.
289	3.91	50.	26.5	10.7	140.	14.3	180.
290	3.73	285.	0.	18.2	1400.	22.1	1700.

Table 3

Transmission T and gyrotron starting current (I) for the three resonators (Table 1).

η is the saturated non-linear single mode efficiency for a 10A annular beam (Table 2).

The static magnetic field B has a taper of 10% over 7.2 cm.

4. MULTIMODE SIMULATIONS

We have simulated the evolution of the TEM modes TEM_{00q} with q = 277-291 by using the computer code described in Ref. [2]. Initially all modes were given an amplitude of 10^{-4} (in normalized units) and random phases. The code was run with the three sets of mode transmissions quoted in Table 3. The multimode behavior of the quasi-optical gyrotron is quite different for stepped and unstepped resonators, as can be seen from Figs. 7a, 7b and 7c. Using mirrors without central step (Fig. 7a) leads after 20 iterations (3.2 μs) to a stationary state where 6 or 7 modes are present. The $TEM_{0\ 0\ 281}$ dominates but the global efficiency, which takes into account the relative phases, is only 14%. Although the evolution is slower, the case of the mirrors with central step is much more interesting. For resonator b, the modes with the lowest starting currents emerge first from noise, and after 5 temporal iterations only the modes q = 283, 285, 287 remain. After 50 iterations (8 μs) a stationary state is reached. For resonator c, it takes about 30 iterations (4.8 μs) until the three modes q = 283, 285 and 287 stand firmly above the background. The mode 285 dominates until iteration 49 but finally all unwanted modes decay, and single mode operation is achieved at around iteration 70 (11.2 μs).

Due to the large amount of CPU time required by these simulations (more than 100'000 s for the last run) only the case with $\Delta B/B = 0.1$ has so far been studied.

5. CONCLUSION

The mode purity of a quasi-optical gyrotron with a large resonator depends crucially on the mirror design. We have shown that mode selection and single mode operation can be achieved by using mirrors with a central step. The resonator formed by such mirrors seems therefore to be a valid solution to the problem of mode selection. Moreover one can take full advantage of the fact that the efficiency increases with the magnetic field taper, without jeopardizing mode purity, contrary to the case of a resonator without step.

It remains to be proved experimentally that stepped resonators exhibiting longitudinal mode selection properties can effectively be manufactured. The construction and passive cavity testing of such a resonator is presently in progress at the CRPP.

Acknowledgments

This work has been partially supported by the Commission pour l'Encouragement de la Recherche Scientifique.

References

1. SPRANGLE, P., VOMVORIDIS, J.L., and MANHEIMER, W.M. 1981, Theory of the quasi-optical electron cyclotron maser. Phys. Rev. A, 23, 3127-3138.

2. BONDESON, A., MANHEIMER, W.M., and OTT, E., 1983, Multimode analysis of quasi-optical gyrotron and gyroklystrons, Infrared and Millimeter Waves, 9, 309-340.

3. HARGREAVES, T.A. KIM, K.J., McADOO, J.H., PARK, S.Y., SEELEY, R.D., and READ, M.E., 1984, Experimental study of a single-mode quasi-optical gyrotron. Int. J. Electron., 57, 977-984.

4. PERRENOUD, A., TRAN, T.M., TRAN, M.Q., RIEDER, C., SCHLEIPEN, M., BONDESON, A., 1984, Open resonator for quasi-optical gyrotrons: structure of the modes and their influence. Int. J. Electron., 57, 985-1002.

5. MATHEWS, H.-G., et al., 1985, Design of a quasi-optical 120 GHz gyrotron. Proceedings of the Course and Workshop on Applications of RF Waves to Tokamak Plasmas, Varenna, Italy, September 5-14, 1985.

6. KREISCHER, K.E. and TEMKIN, R.J., 1983, High-frequency gyrotrons and their application to tokamak plasma heating. Infrared and Millimeter Waves, 7, 377-485.

Figure Captions

Fig. 1: Resonator cross-sections.

a) Conventional spherical mirrors, with output-coupling slot

b) Mirrors with central steps

Fig. 2: Maximum electronic efficiency η_{max} versus w_o/λ for beams with V = 70 kV, $P_\perp/P_\parallel$ = 1.5.

The magnetic field is constant over the intersection region.

(1) Pencil beam.

(2) Annular beam, r_b = 2mm (kr_b = 5.087).

Fig. 3: Resonator output coupling ε versus $|g|$. ($g = 1 - d/R$).

a) T = 0.02

b) T = 0.04.

The resonator is without steps.

Fig. 4: The electronic efficiency η versus electric field E_c at the beam, and the resonator loss divided by IV (parabola) (shown for I = 1, 5, 10A).

Quasi-optical gyrotron operating point (single mode) is at the intersection of two curves:

Resonator : g = -0.2, T = 0.02, d = 36 cm, q = 287

Beam parameters : see Table 2. The magnetic field is constant, B = 4.863 T, $\Delta\omega/\omega$ = 0.035.

Figure Captions (cont'd)

Fig. 5: Contour plots of the electronic efficiency in the (E_C, $\Delta\omega/\omega$) plane for η = 10%, 20%, 30% and loci of the gyrotron operating point for I = 1, 5, 10A.

Resonator: g = -0.2, T = 0.02, d = 36 cm, q = 287.
Beam parameters: see Table 2.
Magnetic field taper is:
a) -0.1, b) -0.05, c) -0., d) 0.05, e) 0.1, f) 0.15.

Fig. 6: Quasi-optical gyrotron operation point (single mode)
The magnetic field has a taper of 10% over 7.2 cm in the interaction region. $\Delta\omega/\omega = 0.026$.

Fig. 7: Multimode evolution of TEM modes 277-291.
Electric field amplitude (normalized units) versus mode number. $E = \sqrt{\pi}\, e\, w_O E_C/(mc^2)$
A time step equals 0.163 μs. η is the global efficiency of all modes. Annular beam parameters: see Table 2. The magnetic field has a taper of 10% over 7.2 cm in the interaction region.

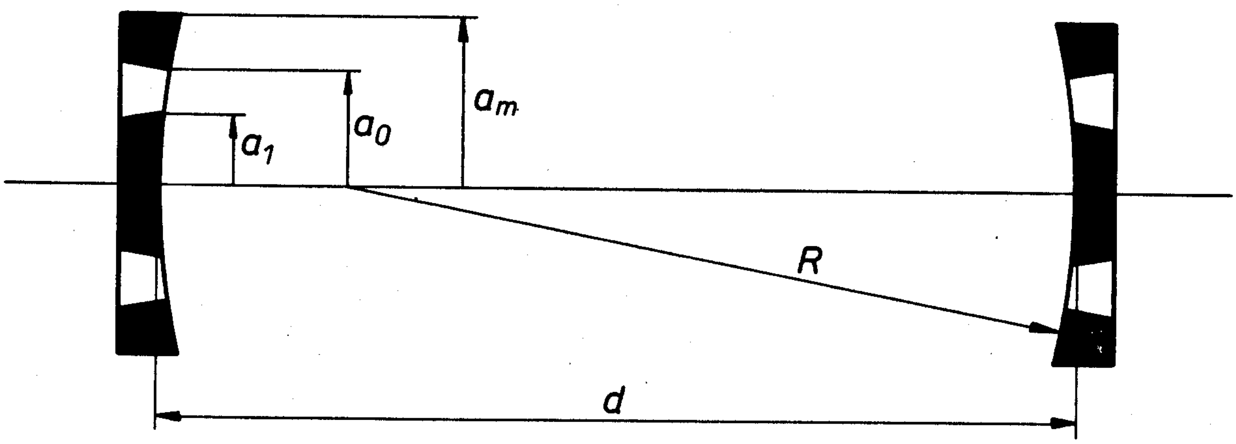

Fig. 1a

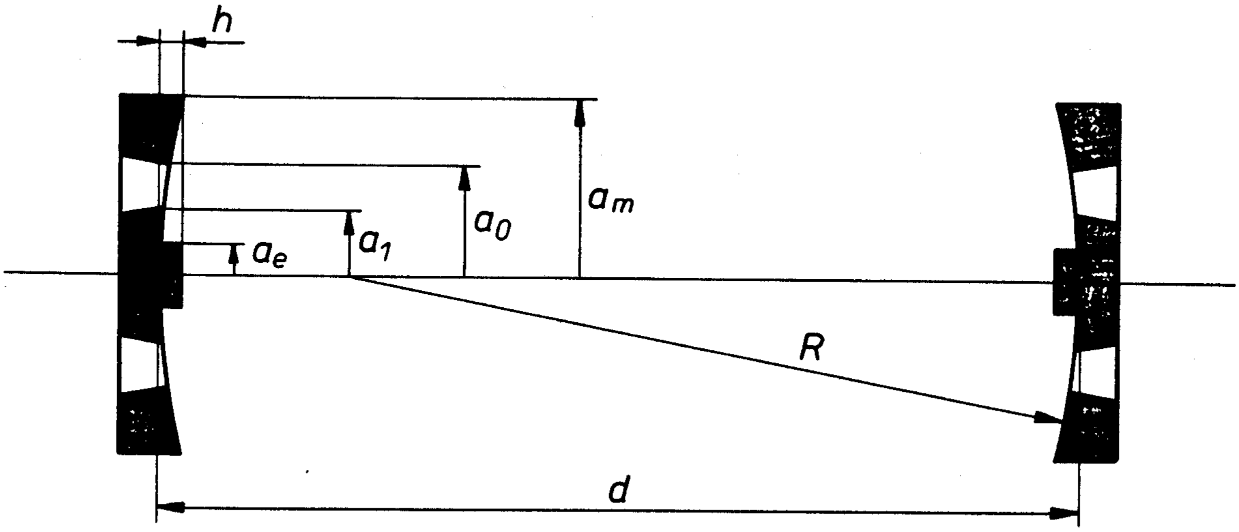

Fig. 1b

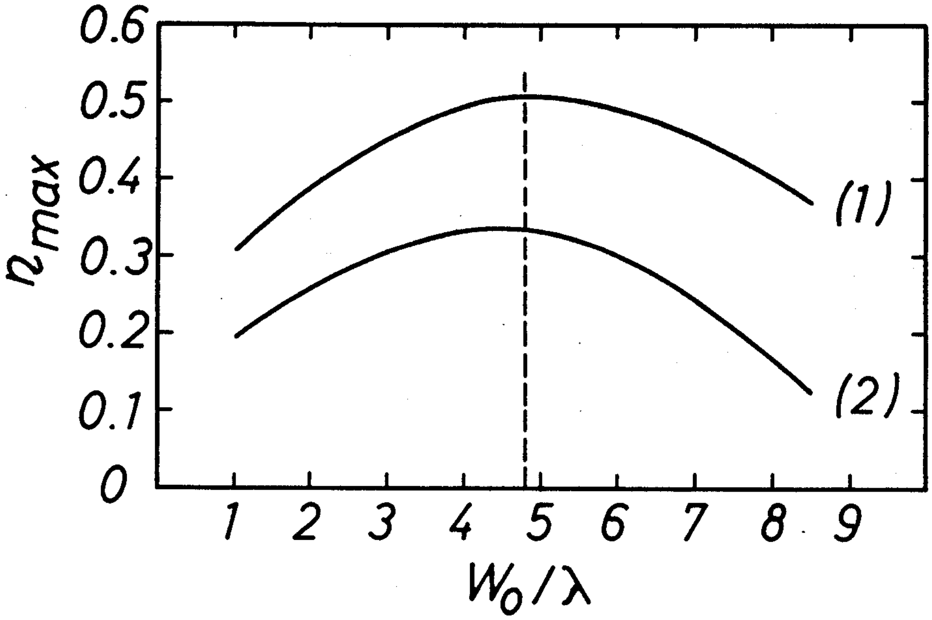

Fig. 2

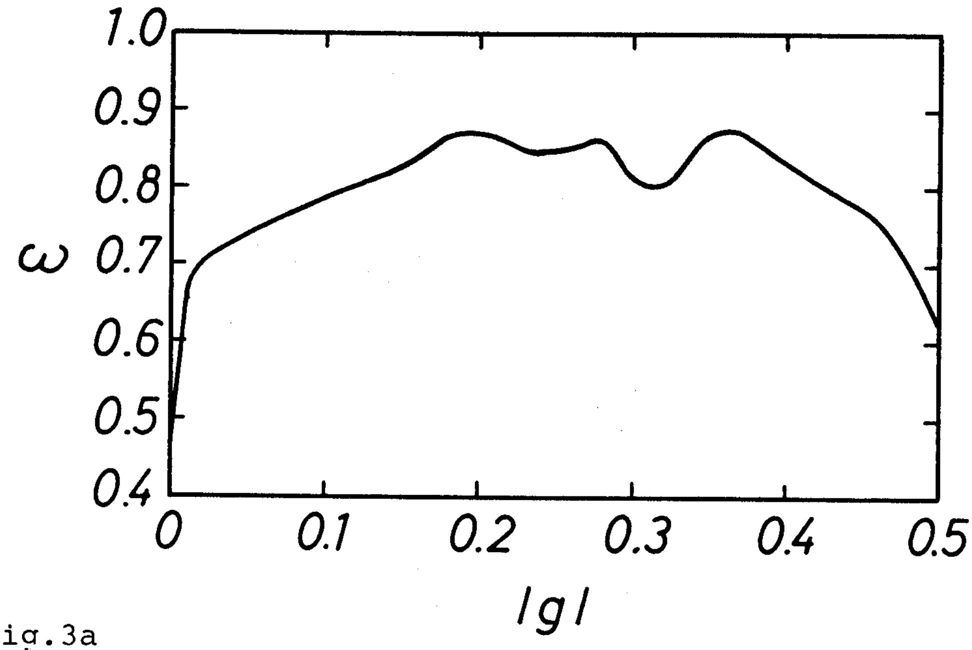
1.0
0.9
0.8
ω
0.7
0.6
0.5
0.4
0
0.1
0.2
0.3
0.4
0.5
|g|

Fig.3a

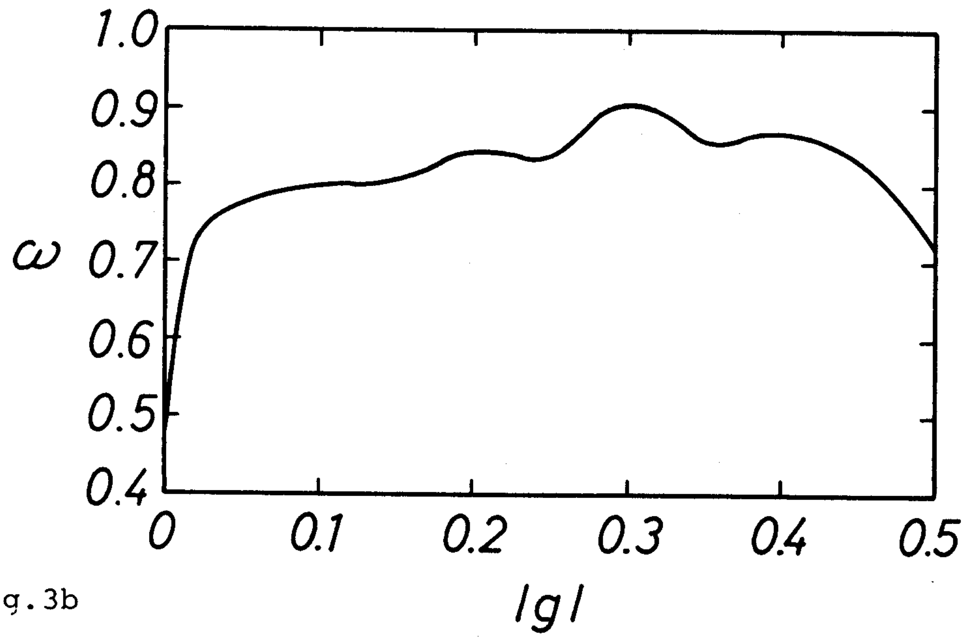
1.0
0.9
0.8
ω
0.7
0.6
0.5
0.4
0
0.1
0.2
0.3
0.4
0.5
|g|

Fig.3b

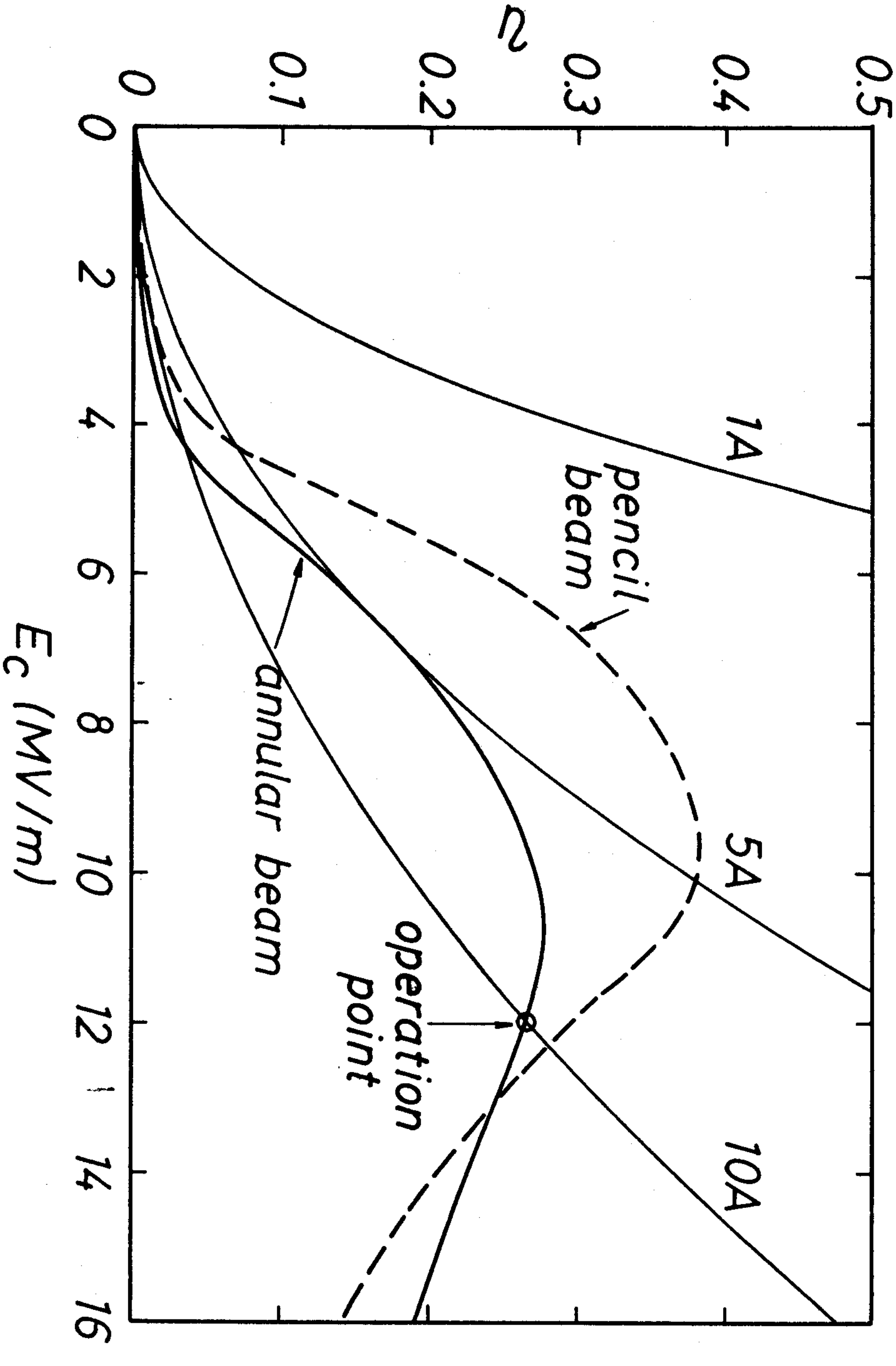
η
0
0.1
0.2
0.3
0.4
0.5
0
2
4
6
8
10
12
14
16
E_c (MV/m)
1A
5A
10A
pencil beam
annular beam
operation point

Fig. 4

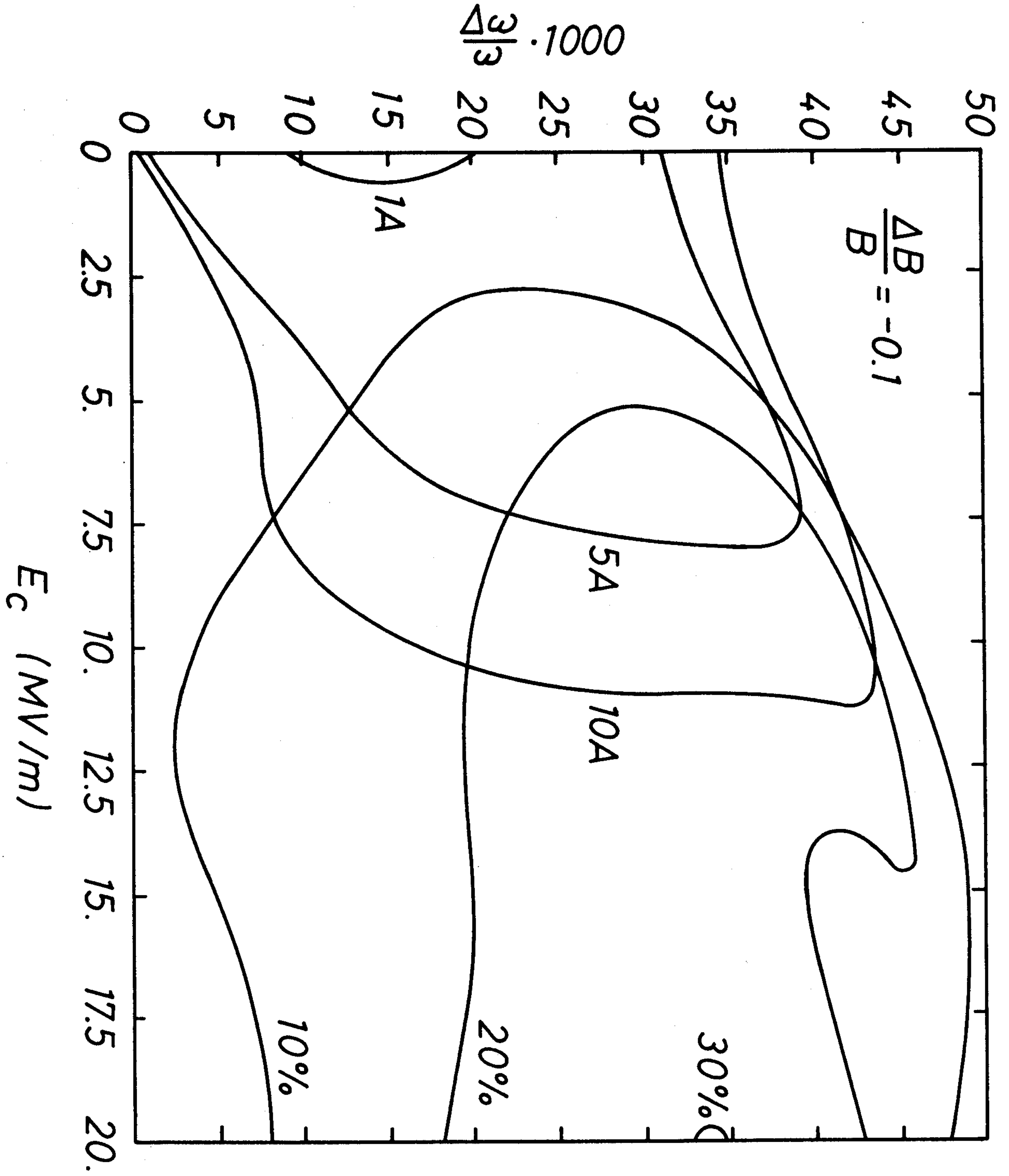

Δω/ω ·1000
0
5
10
15
20
25
30
35
40
45
50
0
2.5
5.
7.5
10.
12.5
15.
17.5
20.
ΔB/B = -0.1
1A
5A
10A
10%
20%
30%
E_c (MV/m)

Fig.5a

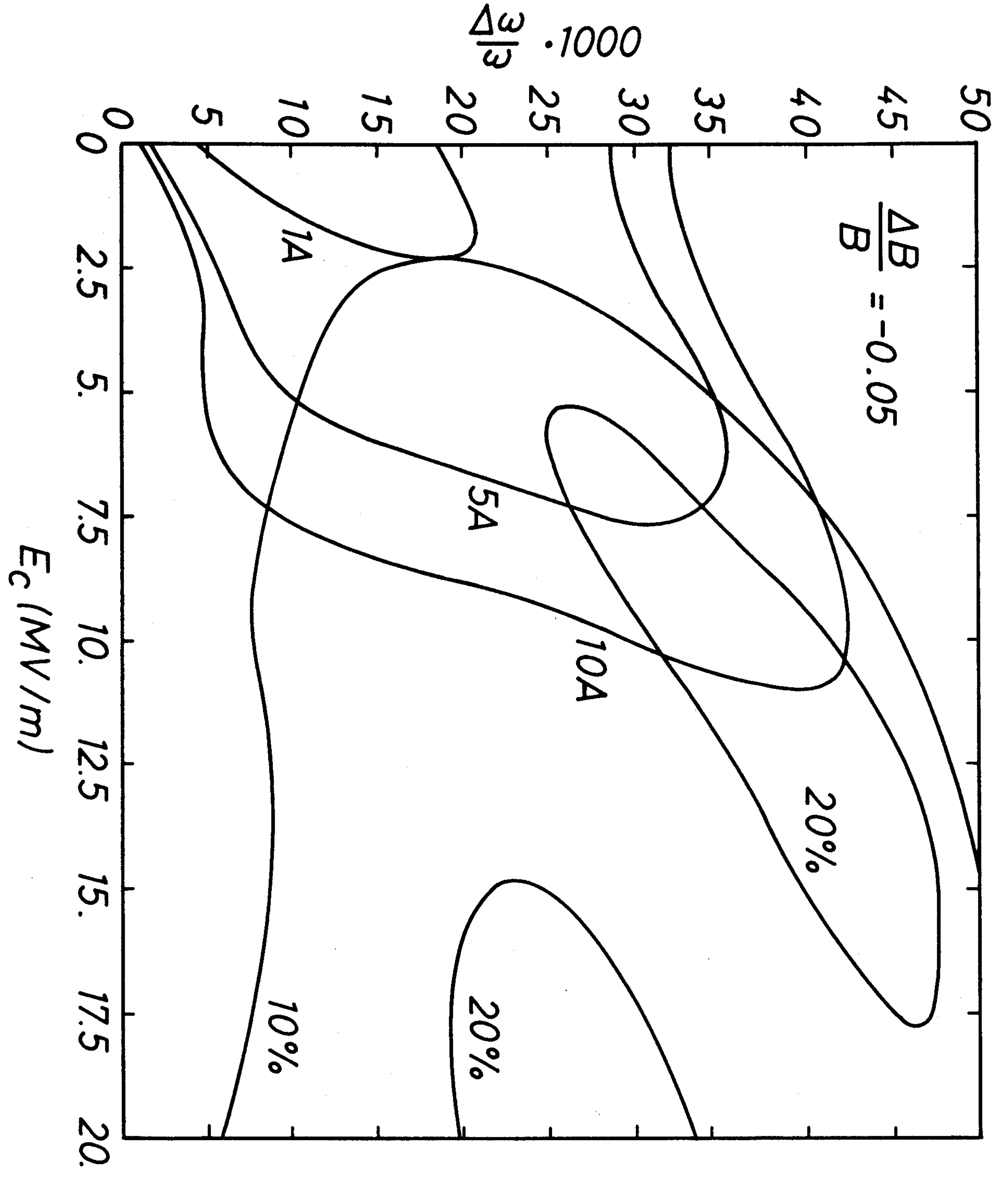

Δω/ω ·1000
ΔB/B = -0.05
0
5
10
15
20
25
30
35
40
45
50
0.
2.5
5.
7.5
10.
12.5
15.
17.5
20.
E_c (MV/m)
1A
5A
10A
20%
20%
10%

Fig.5b

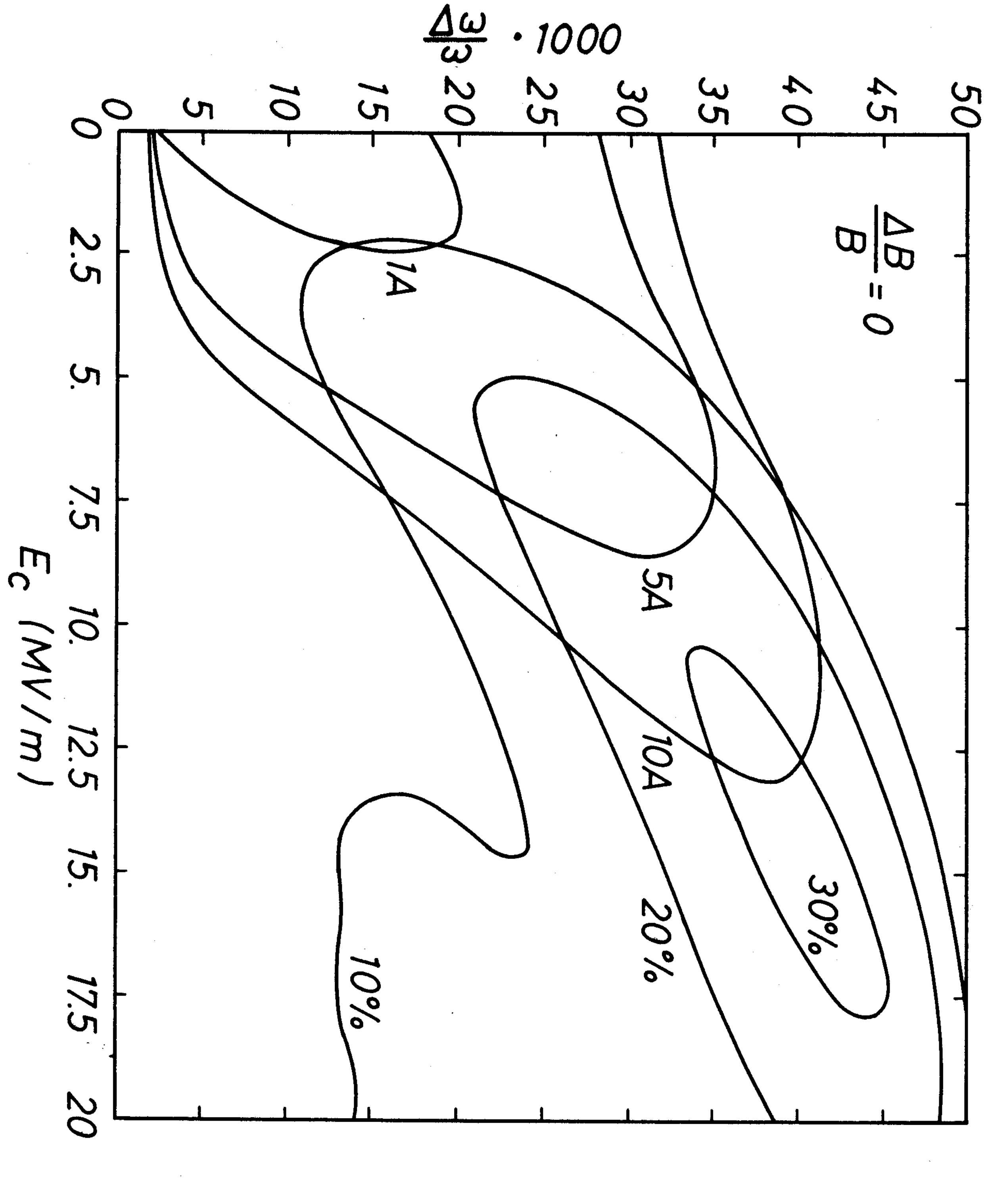

Δω/ω · 1000
ΔB/B = 0
1A
5A
10A
10%
20%
30%
E_c (MV/m)
0
2.5
5.
7.5
10.
12.5
15.
17.5
20
5
10
15
20
25
30
35
40
45
50

Fig.5c

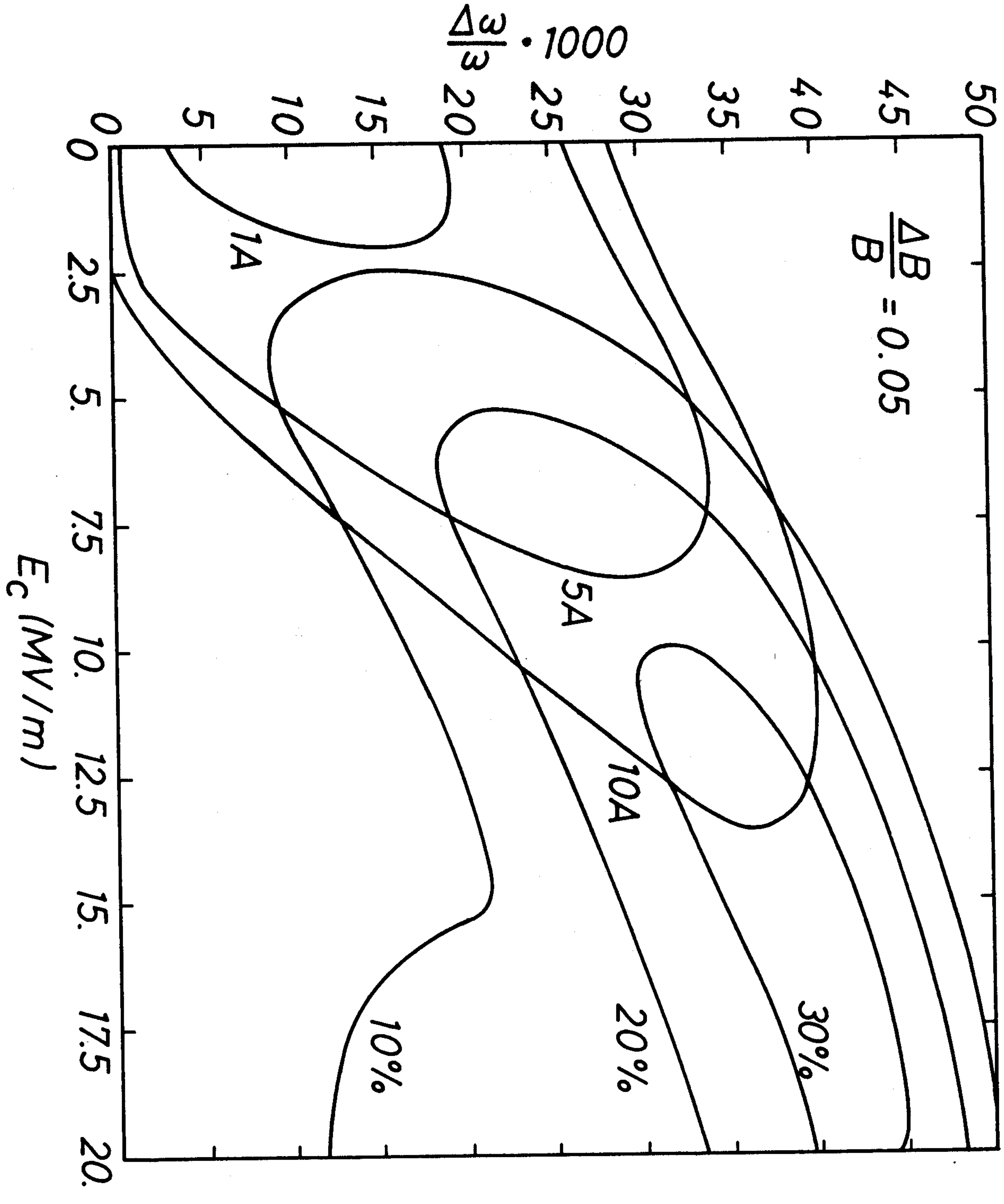
$\frac{\Delta\omega}{\omega} \cdot 1000$
$\frac{\Delta B}{B} = 0.05$
1A
5A
10A
10%
20%
30%
E_c (MV/m)
0
2.5
5.
7.5
10.
12.5
15.
17.5
20.
5
10
15
20
25
30
35
40
45
50

Fig.5d

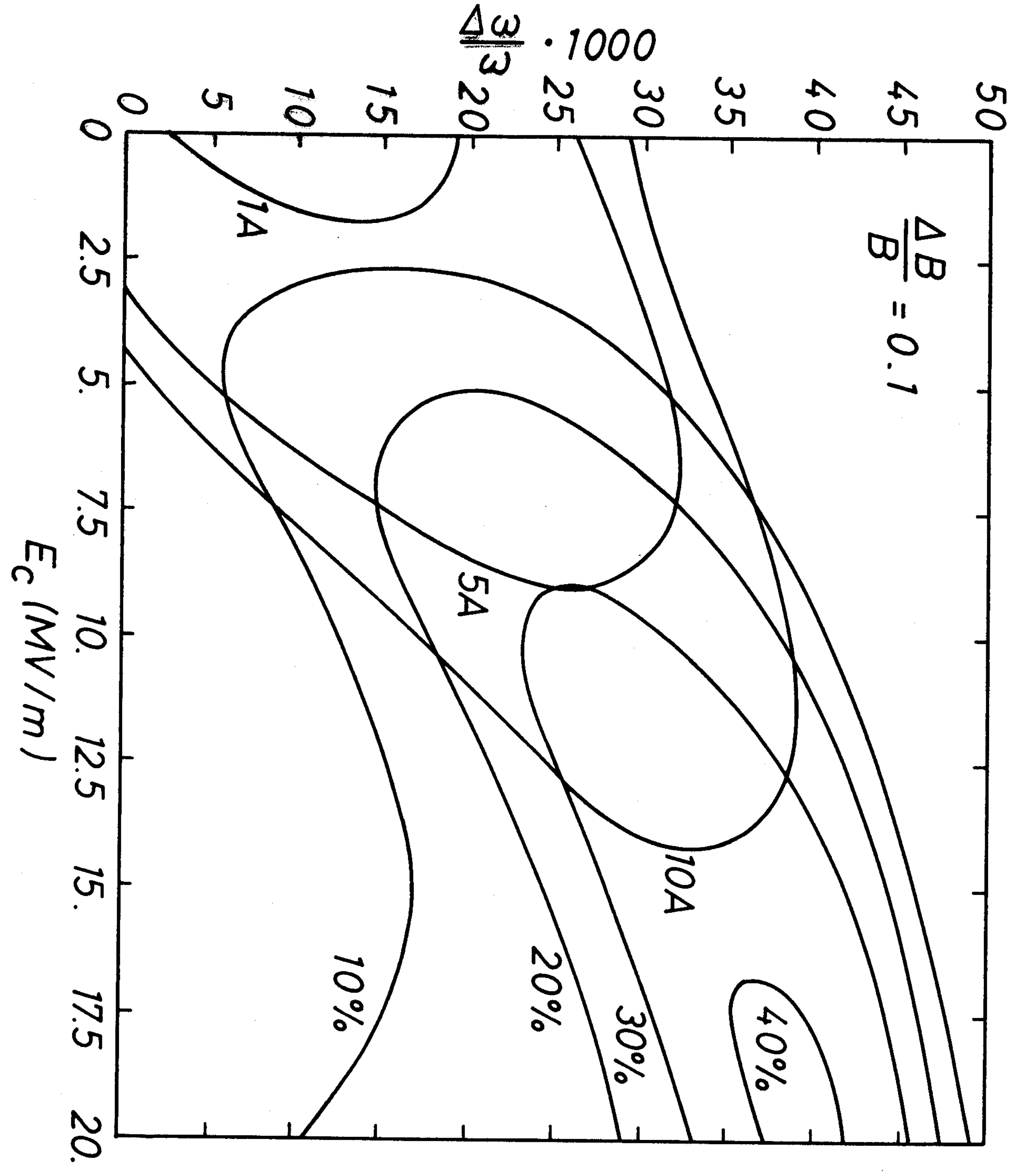

Δω/ω · 1000
0 5 10 15 20 25 30 35 40 45 50
ΔB/B = 0.1
1A
5A
10A
10%
20%
30%
40%
0 2.5 5. 7.5 10. 12.5 15. 17.5 20.
E_c (MV/m)

Fig.5e

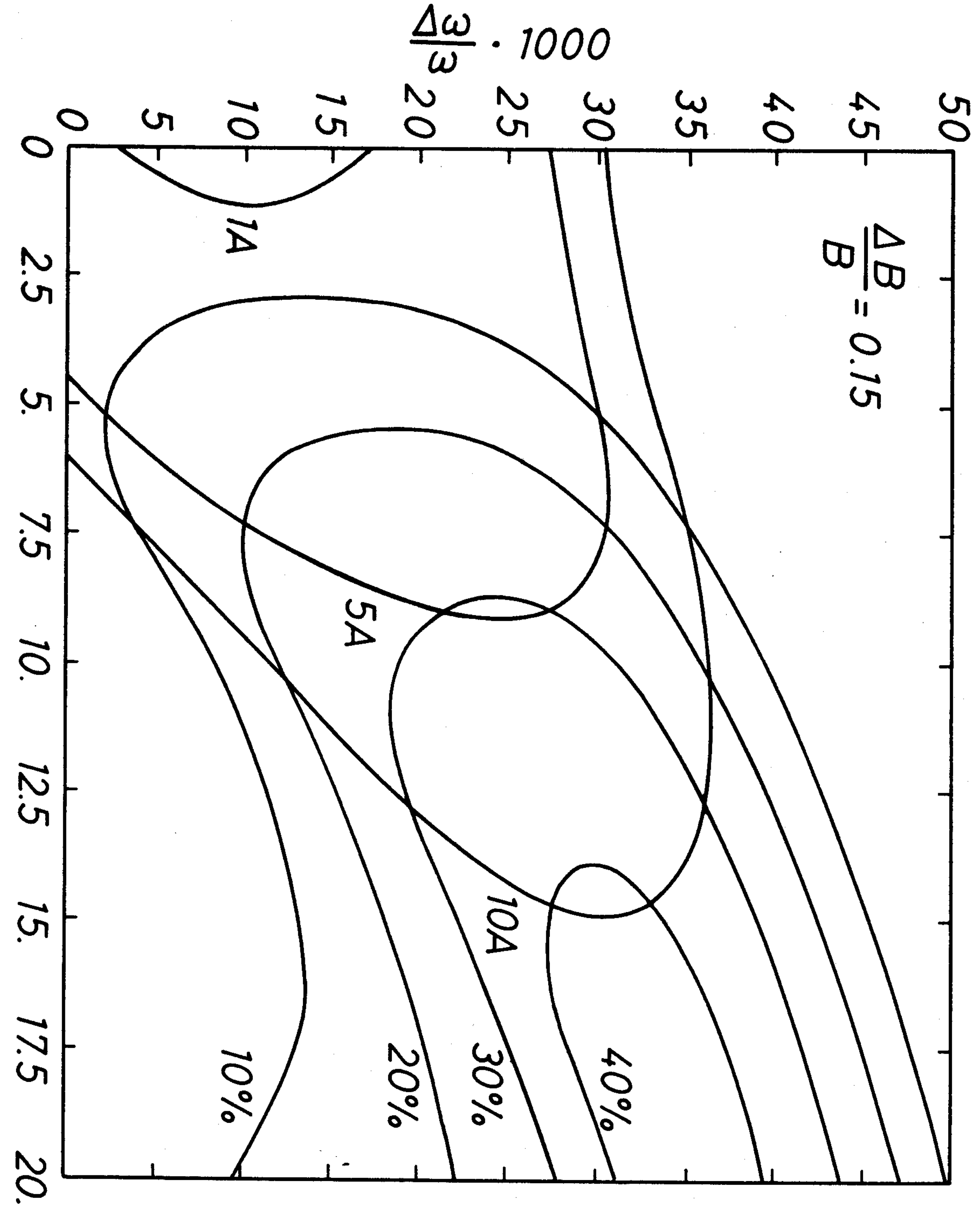

Δω/ω · 1000
ΔB/B = 0.15
0
5
10
15
20
25
30
35
40
45
50
0
2.5
5.
7.5
10.
12.5
15.
17.5
20.
E_c (MV/m)
1A
5A
10A
10%
20%
30%
40%

Fig.5f

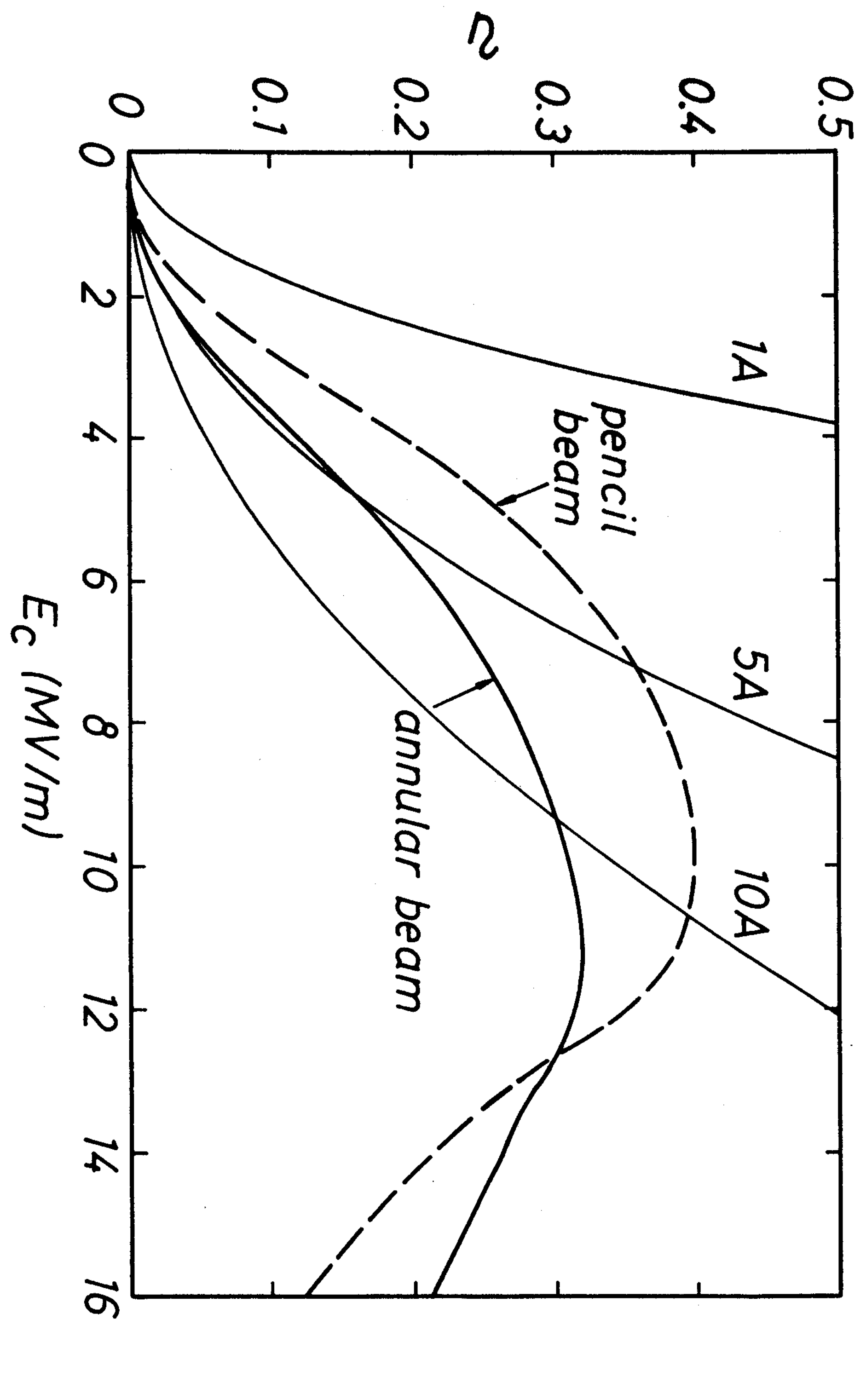

η
0
0.1
0.2
0.3
0.4
0.5
0
2
4
6
8
10
12
14
16
Ec (MV/m)
1A
5A
10A
pencil
beam
annular beam

Fig. 6

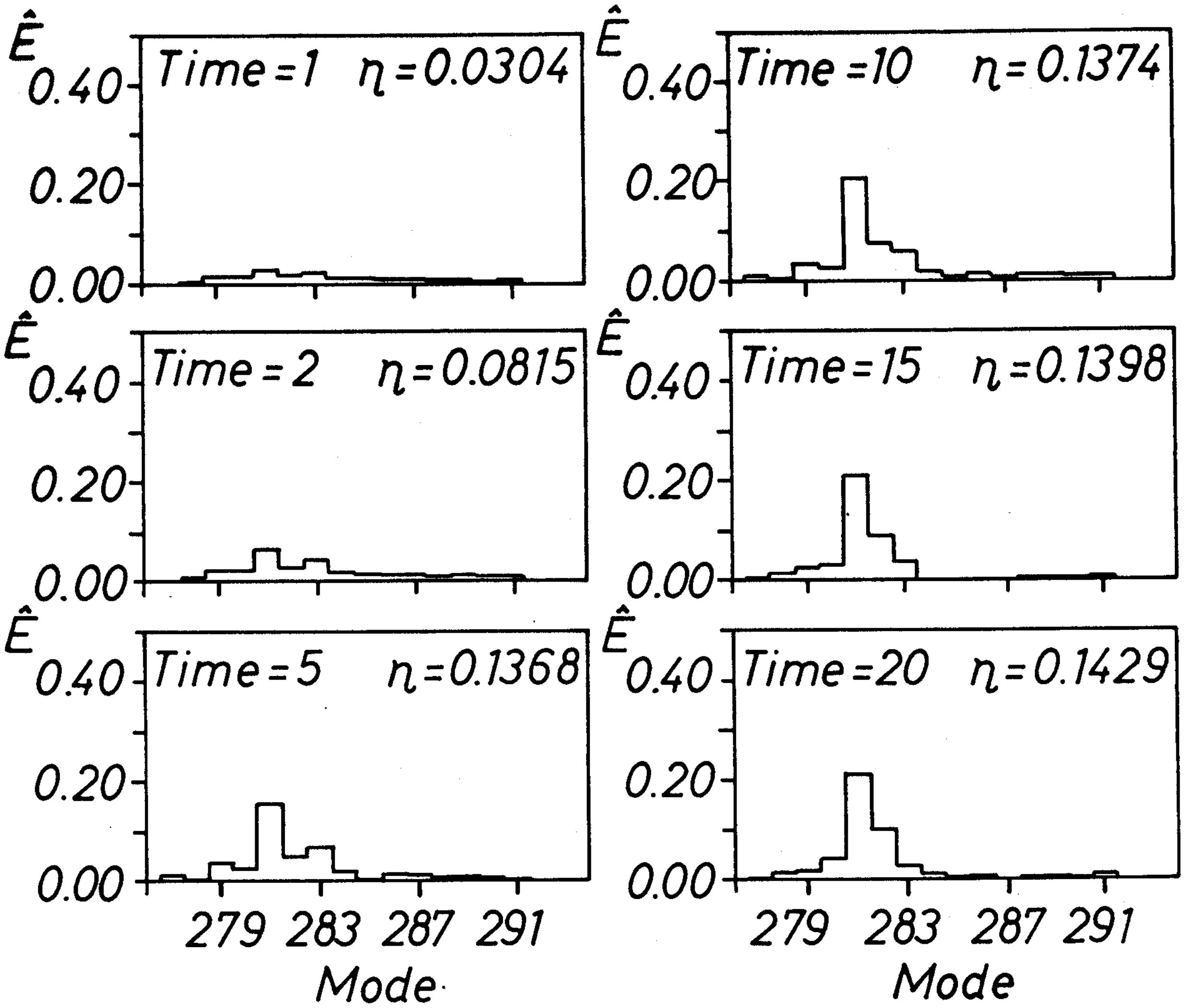

Ê
Time = 1 η = 0.0304
Time = 2 η = 0.0815
Time = 5 η = 0.1368
Time = 10 η = 0.1374
Time = 15 η = 0.1398
Time = 20 η = 0.1429
0.40
0.20
0.00
279 283 287 291
Mode

Fig.7a

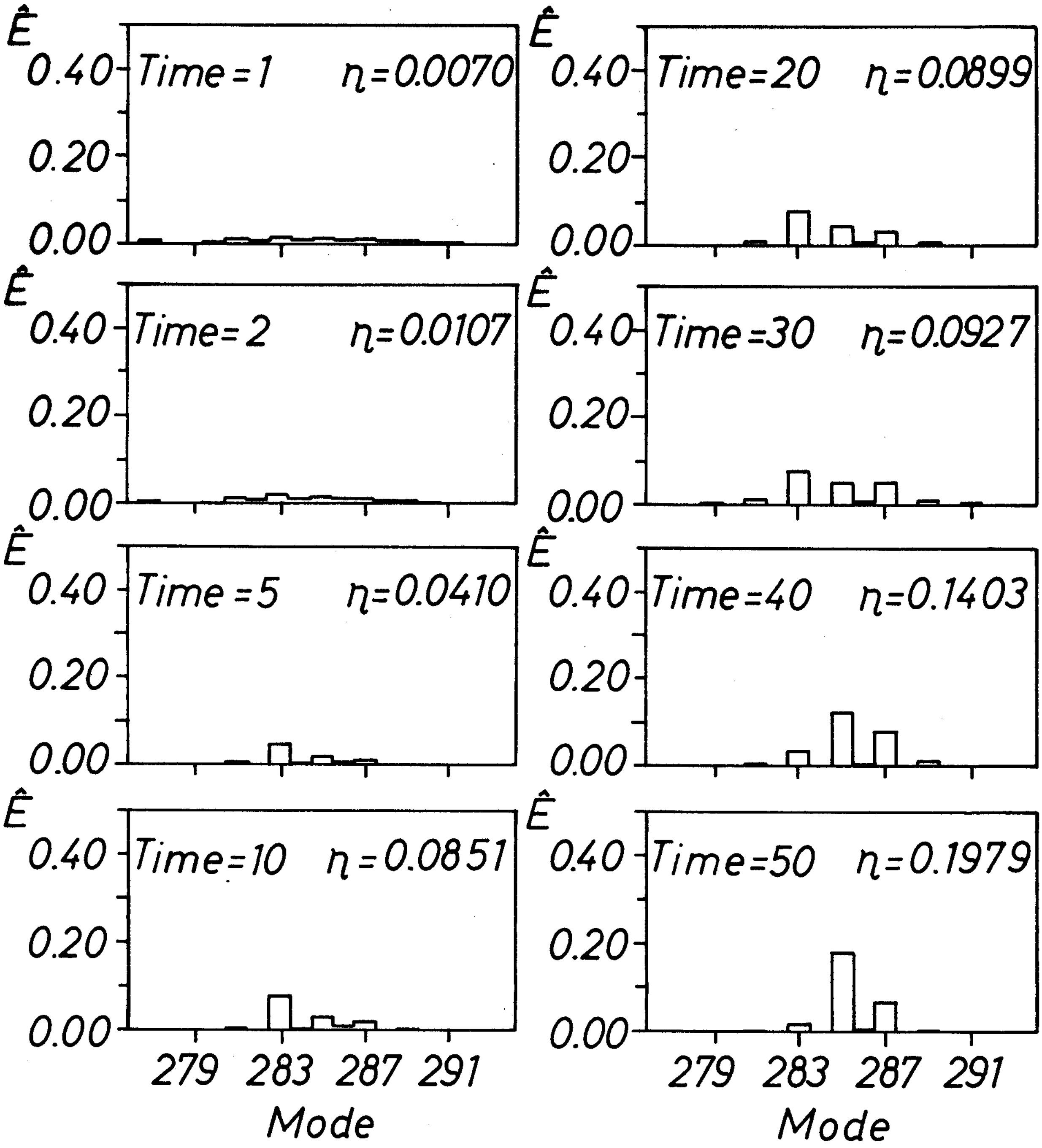

Ê
0.40
0.20
0.00
Time=1
η=0.0070
Time=2
η=0.0107
Time=5
η=0.0410
Time=10
η=0.0851
Time=20
η=0.0899
Time=30
η=0.0927
Time=40
η=0.1403
Time=50
η=0.1979
279
283
287
291
Mode

Fig.7b

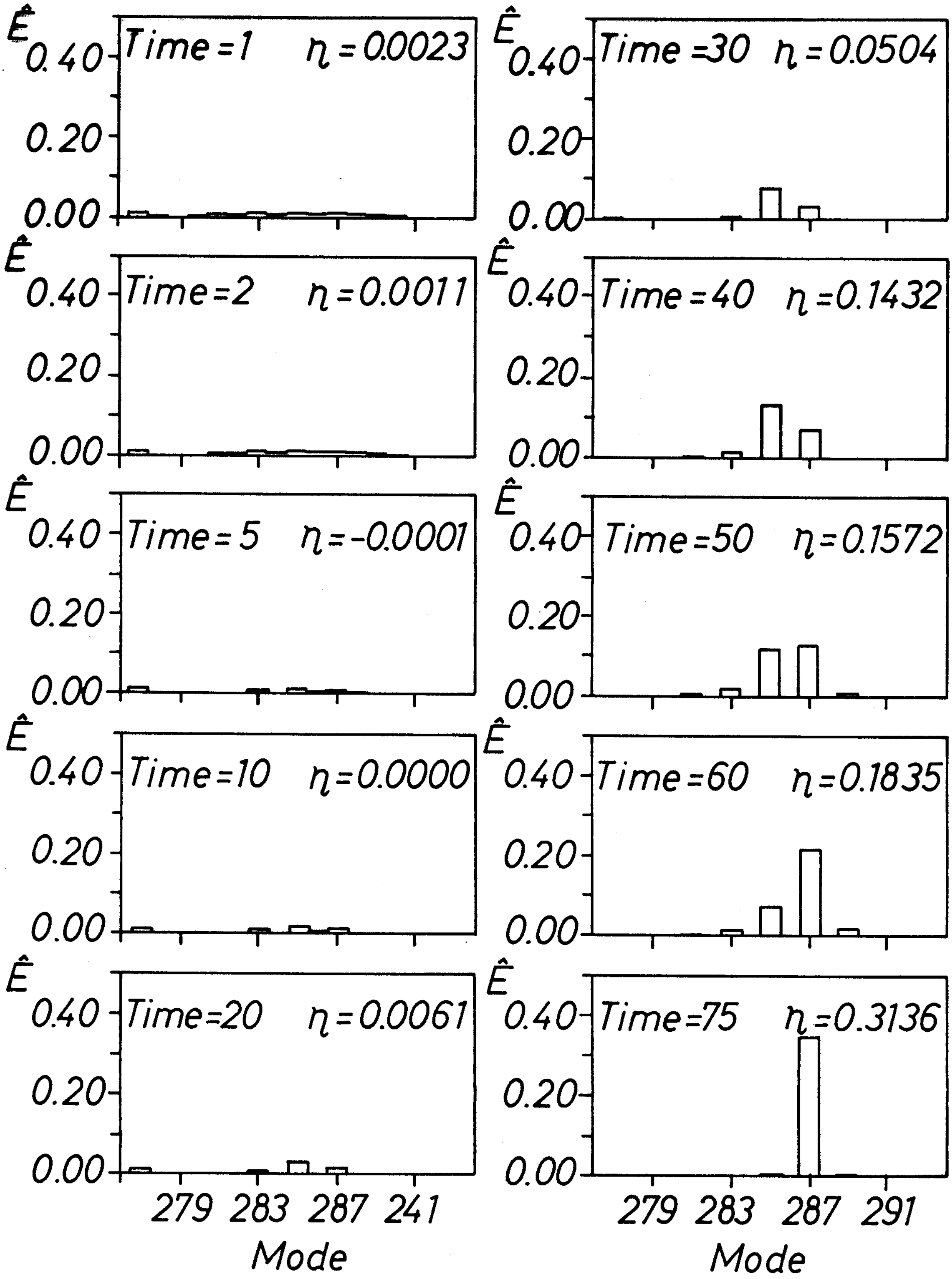
Ê
0.40
0.20
0.00
Time=1 η=0.0023
Time=2 η=0.0011
Time=5 η=-0.0001
Time=10 η=0.0000
Time=20 η=0.0061
Time=30 η=0.0504
Time=40 η=0.1432
Time=50 η=0.1572
Time=60 η=0.1835
Time=75 η=0.3136
279 283 287 241
279 283 287 291
Mode

Fig.7c